Fabrication of TiN Particle-Dispersed Al_2O_3 Composites Utilizing High N_2-Pressure SHS

Ken Hirota*, Hajime Yagura, Katsuya Takaoka, Masaki Kato

Department of Molecular Science and Biochemistry, Faculty of Science and Engineering,
Doshisha University, Kyoto 610-0321, Japan

Abstract

Fabrication of fine TiN particle-dispersed dense Al_2O_3 composites with the compositions of Al_2O_3/TiN=100/0~90/10 vol% has been conducted from Al_2O_3/(Ti,$TiN_{0.3}$) mixed powder compacts by capsule-free hot isostatic pressing (HIP) utilizing high-pressure N_2 SHS. Fine Ti powders (φ ~ 0.3 μm) with $TiN_{0.3}$ phase were prepared by thermal decomposition of planetary ball-milled fine TiH_2 powders at 400°C (673 K) for 1 h in a vacuum, followed by heating in N_2 at 200°C (473 K) for 2 h. The Al_2O_3 powder compacts (relative densities of 57.2-57.8%) with homogeneously dispersed (Ti,$TiN_{0.3}$) particles were prepared. The mixed powder compacts were hot isostatically pressed (HIPed) under the conditions of 1350°C (1623 K) at 7 MPa N_2 for 1 h, followed by the heating at the same temperature for 2 h under 196 MPa-N_2. At the first stage of heating [1350°C (1623K)/7MPa/1h], solid/gas reaction of SHS between (Ti,$TiN_{0.3}$) and N_2 was introduced to form TiN and densification of the Al_2O_3 powder compacts up to the relative density of 92-93% with closed pores was performed. And at the sequent second stage [1350°C (1623K)/196MPa/2h], densification of the most of pre-sintered composites consisting of Al_2O_3 and TiN reached higher relative densities than 98.5%. Dispersion of TiN particles (~φ 0.30 μm) in the composites suppressed the grain growth of Al_2O_3 during HIP-sintering. Mechanical properties, such as bending strength (σ_b), Vickers hardness (H_V), fracture toughness (K_{IC}), and electrical resistivity (ρ) of the composites were evaluated as a function of TiN content; the maximum values of σ_b=640 MPa, H_V=19.5 GPa, and K_{IC}=4.5 MPa・$m^{1/2}$ were obtained in the Al_2O_3/TiN=97/3~95/5 vol% composites. Among the composites, the lowest ρ value of 2.6×10^3 Ω・m was attained at Al_2O_3/TiN=90/10 vol% composite.

Introduction

Metal nitrides reveal often desirable combined properties, such as high melting temperatures, high hardness, low density (light weight), low electrical resistivity, excellent wear resistance and high chemical stability. Therefore, they have been widely used in semiconductor industries and other applications. Among them, titanium nitride (TiN) shows excellent properties and it has been attracting increasing interest as a constituent of composites for widely applications, such as cutting tools, tool coating, microelectronics [1], and solar-control films.

A lot of research-papers concerning on Al_2O_3/TiN composite materials have been published, and many of them treated the sintering of mixtures of Al_2O_3 and TiN powders [2-4]. In general, TiN powders commercially available consist of large particles because TiN cannot be crushed into fine powders with a conventional milling process due to its excellent high hardness. Therefore, the addition of large TiN particles to other matrix materials often resulted in reduction of original mechanical properties, and their improvement in the performance of composite materials cannot be expected. Therefore, fine TiN particles are required to fabricate dense TiN-added composites with excellent mechanical properties. However, metal Ti powders as starting material for TiN cannot be crushed by conventional ball-milling process because of its high ductility. It was reported

*corresponding author. Email: khirota@mail.doshisha.ac.jp

 Printed in Kazakhstan

that fine metal Ti powders were prepared by the reduction of metal oxides, such as, heat-treatment of fine TiO_2 powder under nitrogen [5] or NH_3 [6].

In the present study to prepare fine metal Ti powders, brittle TiH_2 was chosen as starting material, because this compound can be mechanically crushed. Submicron-meter size ($Ti,TiN_{0.3}$) powders were produced by heating ball-milled TiH_2 in a vacuum. $Al_2O_3/(Ti,TiN_{0.3})$ mixed powder compacts were fabricated, in which thus obtained fine ($Ti,TiN_{0.3}$) powers were uniformly distributed in the Al_2O_3 powders. And moderate nitrogen-pressure was applied at the first stage of HIP sintering in order to both transform ($Ti,TiN_{0.3}$) to TiN by SHS phenomenon of TiN and sinter the powder compacts to a nearly 92~93% relative density without using a gas-tight metal or glass capsule (can). Then, at the sequent second stage of HIP sintering high pressure N_2 densified the pre-sintered bodies to the almost full-density. This capsule-free HIPing method at one time has many merits from industrial view points, for example, low production cost, free-selection of shape and size of the sintered compacts without pre-sintering of green bodies. This capsule-free high-pressure N_2 HIPing can also make it possible that metal nitrides can be formed, even though this metal cannot be nitrided under atmospheric N_2 pressure at high temperatures. Simultaneous synthesis of titanium nitride directly from Ti and the mechanical properties of the fine TiN particles-distributed Al_2O_3 composites were described in relation with their microstructures.

Experimental

Preparation of TiH_2 powder

Starting powder was TiH_2 (TSHT, Osaka Titanium Technologies Co. Ltd, Hyogo, Japan, particle size $P_s \leq 45$ μm, ~99.98% purity). Two kinds of pulverization methods were employed to crush or mill the brittle powder, and the grinding capability difference between them was compared. One pulverization method was that the powder was crushed with a planetary ball mill (*P-5*, Fritsch Japan, Yokohama, Japan) using stainless-steel SUS balls (φ10 mm in diameter) for 100 h at a rotating speed of 200 rpm (centrifugal force about ~ 4.36 *g*: here, "*g*" is a gravitational acceleration unit) with a milling media *vs*. powder ratio of 10:1 in Ar. The other pulverization method was that after crushing with a mortar and pestle for 20 minutes then the powder was milled with a planetary ball mill (*P-5*, Fritsch Japan) using tungsten carbide WC balls (φ5 mm in diameter) for 3 h at 300 rpm (~12.1 *g*) in Ar. And then the powder was further ground with a planetary ball mill (*Premium Line P-7*, Fritsch Japan) using partially stabilized zirconium (PSZ) balls (φ1 mm in diameter) for 10 min at 1100 rpm (~83.9 *g*) in ethyl-alcohol and Ar.

Preliminary experiment to determine the crystalline phase of dehydrated TiH_2 powder

Ball-milled TiH_2 powders were dehydrated by heating at 400°C (673 K) for 1 h in a vacuum and a sequent heating at 200°C (473 K) for 1 h in N_2. The crystalline phase of powders after the dehydrations was identified by X-ray diffraction (XRD) analysis (Cu*K*$\alpha_1$radiation with a graphite monochromator, *Rint 2000*, Rigaku, Osaka, Japan). As will be described later, the powders after dehydration heat-treatment gave the Ti (JCPDS#44-1294) or $TiN_{0.3}$ (JCPDS#41-1352) phases; Ti phase was obtained via ball-milling with SUS balls, on the other hand, $TiN_{0.3}$ phase was prepared via a combined ball-milling process with WC and ZrO_2 (PSZ) balls. This might be explained in terms of reactivity difference in ball-milled TiH_2; a combined ball-milling with smaller WC and ZrO_2 (PSZ) balls produced higher reactive powders than those from larger SUS balls.

Fabrication of Al_2O_3/TiN composites by capsule-free N_2-HIPing

After ball-milling, TiH_2 powder (average particle size P_s ~ 0.3 μm) and fine α-Al_2O_3 powder (TM-DAR, Taimei Chemicals Co. Ltd, Nagano, Japan, P_s ~ 0.10 μm, ~99.99 % purity) were weighed into $Al_2O_3/(Ti,TiN_{0.3})$=100/0 ~ 90.7/9.3 vol%, by assuming that all Ti and $TiN_{0.3}$ powders would transform into TiN after the heat-treatment under moderate nitrogen pressures (about 4-7 MPa) at high temperatures (about 1373-1473 K) by SHS between (Ti, $TiN_{0.3}$) and N_2 and then the composite powders would have the compositions of Al_2O_3/TiN =100/0 ~ 90/10 vol%. The powders of Al_2O_3 and milled TiH_2 were mixed with a mortar and pestle for 1 h in Ar. Then, the mixed powders were treated by thermal decomposition at 400°C (673 K) for 1 h in a vacuum, followed by the thermal treatment at speed of 700 rpm (a centrifugal force about ~11 *g*. Then, the powders were dried at 80°C (353 K) in a vacuum for 6 h and

then cooled in Ar. The dry mixed powder was compacted using an uniaxial metal mold/plunger (φ13 mm in diameter) at 20 MPa and then, densified by cold isostatic pressing (CIP) at 245 MPa for 1 min. Mixed powder $Al_2O_3/(Ti,TiN_{0.3})$ compacts were HIP-treated. Dense Al_2O_3/TiN composites were fabricated by capsule-free N_2-HIPing [1350°C (1623 K)/7MPa/3.6×10^3s(1h) +1350°C (1623 K)/196 or 98 MPa/7.2×10^3s(2h)]; this conditions were determined by the results obtained from our preliminary experiments.

Characterization of samples

Crystalline phases of samples were identified by X-ray diffraction (XRD) analysis as described above. Bulk densities of the powder compacts and sintered samples were evaluated by measuring weights/dimensions and Archimedes methods, respectively. As-received and ball-milled powders and microstructure observation on the fractured or polished surfaces of sintered composites was performed using a field emission-type scanning electron microscope (FE-SEM, *JSM-7001FD*, JEOL, Tokyo, Japan) equipped with an energy-dispersive spectroscope (EDS, *JED-2300/F*, JEOL) and their average grain sizes were determined by an intercept method [7]. A field emission-type transmission electron microscope (FE-TEM, *JEM-2100F*, JEOL) equipped with an energy-dispersive spectroscope (EDS, *JED-2300/F*) were also utilized to observe the morphology, analyze the elemental distribution, and examine the electron diffractions on the nano-regions of the composites. Before TEM observation, the specimens were made thinner using a focused ion beam (FIB, *FB-2000A*, Hitachi High-Tech Fielding) equipped with a micro-sampling system.

After crystalline phase identification, test bars (~3×3.5×11 mm^3) for mechanical-property measurements were cut from the sintered materials with a diamond cutting-blade and then their four sides were polished to mirror surface with a diamond paste (nominal particle size 1-3 μm). Three-point bending strength (σ_b) was evaluated with a cross-head speed of 0.5 mm/min and an 8 mm-span length using WC jigs. Vickers hardness (H_v) and fracture toughness (K_{IC}) were evaluated with an applying load of 19.6 N and a duration time of 15 s for the former, and the indentation fracture method (IF) with Niihara's equation for the latter [8].

Direct current (DC) electrical resistivity (ρ) of composites were measured at room temperature by Ag four-terminal (1.0 mm intervals) method with a programmable DC voltage/current source and a multifunctional-volt meter.

Results and Discussion

Characterization of fine Ti powders

Figure 1 shows SEM photographs of TiH_2 powders; (a) as-received, (b) and (c) are the photographs of powders after ball milling using SUS balls (10 mm^{Φ}) for 100 h in Ar (4.36 *g*) and after combined ball milling process using WC balls (5 mm^{Φ}) for 3 h in Ar (12.1 *g*) & ZrO_2 balls (1 mm^{Φ}) for 10 min in ethanol (83.9 *g*), respectively. These photographs reveal that the starting material of TiH_2 composed of small and large crushed particles up to around 8 μm, and the particle sizes of ball-milled powders were about 0.3 μm. It should be noted that the combined ball milling, *i.e.*, WC balls (5 mm^{Φ}) for 3 h in Ar (12.1 *g*) + ZrO_2 balls (1 mm^{Φ}) for 10 min in ethanol (83.9 *g*), gave the

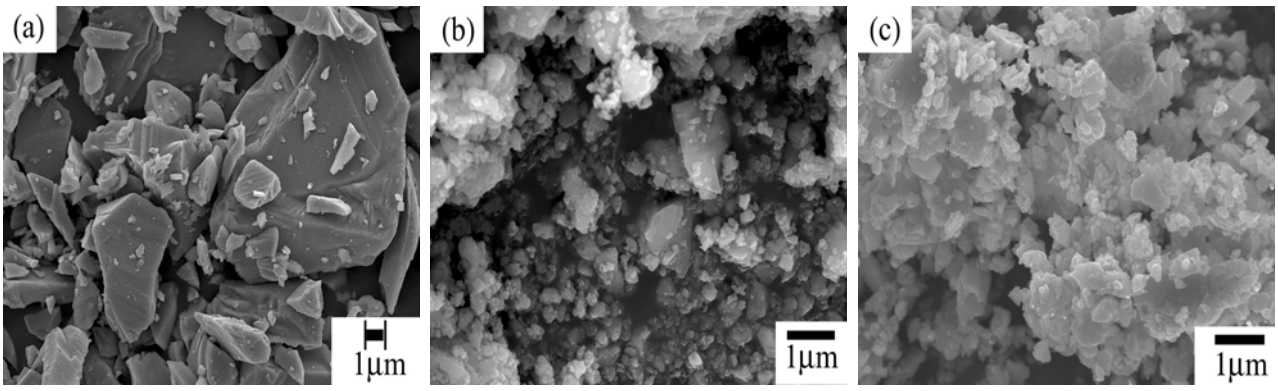

Fig. 1 FE-SEM photographs of TiH_2 powders; (a) as-received, (b) and (c) are the photographs of powders after ball milling using SUS balls (10 mm^{Φ}) and after combined ball milling process using WC balls (5 mm^{Φ}) & ZrO_2 balls (1 mm^{Φ}), respectively.

homogeneous fine powders without agglomeration (~8 μm) as observed in the powder milled with large SUS balls (10 mm^{Φ}). This might be explained by that during the (SUS-ball) milling sufficient energy for pulverization was not supplied due to both dry pulverization process and low density of SUS balls (0.77 Mg/m^3) under the centrifugal force about 4.36 *g*, even though long duration time up to 100 h. On the other hand, in the combined ball-milling process, heavy large WC balls (15.66 Mg/m^3, 5 mm^{Φ}) milled the coarse particles in dry-process moderately (3 h) and then light small ZrO_2 (PSZ) balls (6.05 Mg/m^3, 1mm^{Φ}), with high milling energy due to the centrifugal force of 83.9 *g* from a high rotating speed of 1100 rpm, ground the pre-milled powders down to 0.3 μm, deflocculating the fine particles in ethy-alchol.

Figure 2 shows XRD patterns of the TiH_2 powders (a) after ball milling using SUS balls and (b) prepared from the combined milling process. In Fig. 2(a), main XRD peaks of $TiH_{1.924}$ (JCPDS#25-0982) and a small amount of Ni-Cr-Fe (JCPDS#35-0983) phases were observed; the latter impurity phase was originated from the SUS vessel and balls during milling. On the other hand, as WC and ZrO_2 (PSZ) balls with excellent wear resistance were used for the second pulverization process, impurities were not observed in the XRD pattern.

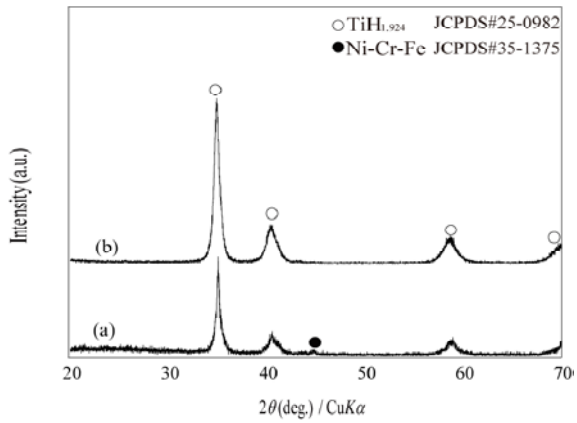

Fig. 2 XRD patterns of the TiH_2 powders (a) after ball milling using SUS balls and (b) prepared from the combined milling process.

Then the microstructure of mixed powder (Al_2O_3/[Ti/$TiN_{0.3}$]) compacts thus fabricated was observed. Figure 3 shows FE-SEM photographs for the fracture surfaces of powder compacts corresponding to Al_2O_3/TiN=90/10vol% composition prepared from Al_2O_3 and the Ti/$TiN_{0.3}$ powders. Here, Ti/$TiN_{0.3}$ were prepared by dehydration of the TiH_2 powder milled using: (a) SUS balls (10 mm^{Φ}) and (b) WC balls (5 mm^{Φ}) & ZrO_2 balls (1 mm^{Φ}). It was observed that white particles of (Ti/$TiN_{0.3}$ particles) were distributed homogeneously in the black Al_2O_3 powder matrix in both cases. Bulk densities of mixed powder compacts increased monotonously from 2.28 to 2.34 Mg/m^3 with increasing Ti/$Ti_{0.3}$ content as shown in Table 1. Inversely, relative densities calculated from the theoretical densities (3.987, 4.503 and 4.715 Mg/m^3) of Al_2O_3 (JCPDS#46-1212), Ti (JCPDS#44-1294) and $TiN_{0.3}$ (JCPDS#41-1352), respectively, increased a little from ~57.2 to ~57.8%. In calculation of their theoretical density, the density of impurities was ignored due to its small amount.

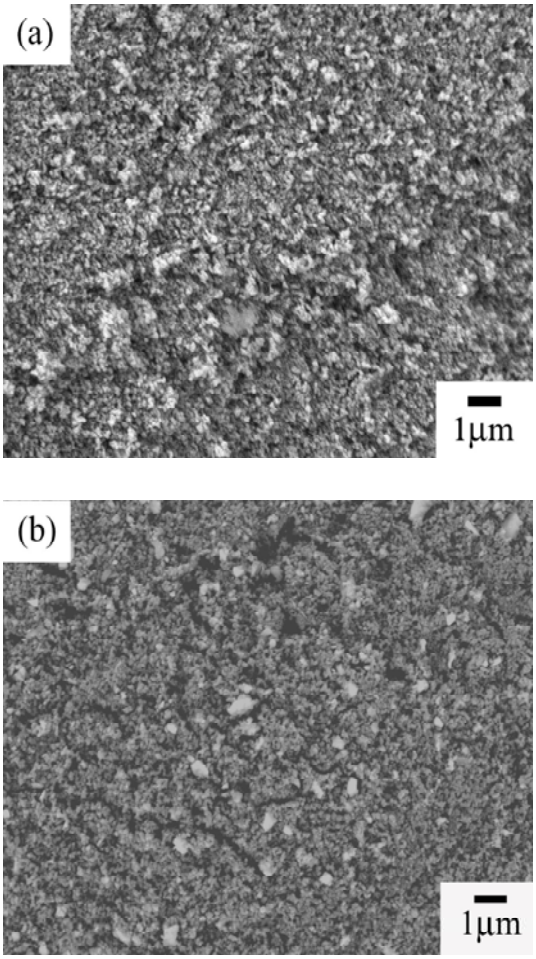

Fig. 3. FE-SEM photographs for the fracture surfaces of powder compacts corresponding to Al_2O_3/TiN=90/10 vol% composition prepared from Al_2O_3 and the Ti/$TiN_{0.3}$ powders. Here, Ti/$TiN_{0.3}$ were prepared by dehydration of the TiH_2 powder milled using: (a) SUS balls (10 mm^{Φ}) and (b) WC balls (5 mm^{Φ}) & ZrO_2 balls (1 mm^{Φ}).

Table 1

Bulk and relative densities of mixed powder compacts fabricated using CIP (245 MPa) from dehydrated powders which were ball-milled with: (a) SUS ball (10mm$^{\Phi}$) for 100 h in Ar (4.36 *g*) and (b) a combined milling process of WC ball (5 mm$^{\Phi}$) for 3 h in Ar (12.1 *g*) & ZrO_2 ball (1 mm$^{\Phi}$) for 10 min in ethanol (83.9 *g*) and Ar.

(a)

Compositions of HIP-sintered materials Al_2O_3/TiN (vol%)	Densities of powder compacts		
	Bulk density (Mg/m^3)	Theoretical density* (Al_2O_3/Ti vol%) (Mg/m^3)	Relative density (%)
100/0	2.28	3.987	57.1
99/1	2.27	3.992	56.8
97/3	2.30	4.001	57.6
95/5	2.31	4.011	57.6
93/7	2.33	4.021	58.0
90/10	2.34	4.035	58.0

(b)

Compositions of HIP-sintered materials Al_2O_3/TiN (vol%)	Densities of powder compacts		
	Bulk density (Mg/m^3)	Theoretical density* ($Al_2O_3/TiN_{0.30}$) (Mg/m^3)	Relative density (%)
100/0	2.30	3.987	57.6
95/5	2.25	4.021	55.9
90/10	2.22	4.055	54.8

*Theoretical densities of Dx(Al_2O_3:JCPDS#46-1212) = 3.987, D_x(Ti: JCPDS#44-1294) = 4.503, and D_x($TiN_{0.3}$: JCPDS#41-1352) = 4.715 Mg/m^3 were used.

Microstructure of Al_2O_3/TiN composites

After the 1st stage of HIPing [1350°C(1623K)/7MPa/3.6×10^3s(1h)] shown in Fig. 4, the samples corresponding to the compositions of Al_2O_3/TiN=100/0, 95/5, and 90/10 vol% were taken out from HIP apparatus and then evaluated from viewpoints of the crystalline phase change, microstructure development and the bulk densities. XRD patterns of the pre-sintered bodies revealed that the materials consisted of Al_2O_3 and TiN with a small amount of $Al_{0.54}Ti_{2.46}N_{0.28}O_{4.58}$ (JCPDS#42-1279), proving that the formation of TiN by solid/gas reaction between (Ti/$TiN_{0.3}$) and 7 MPa-N_2. Their relative densities were determined to be 97.5% (Al_2O_3/TiN=100/0 vol%, bulk density of 3.89 Mg/m^3), 95.5% (95/5 vol%, 3.87 Mg/m^3), and 94.5% (90/10 vol%, 3.90 Mg/m^3) based on the theoretical densities of crystalline phases for Al_2O_3 (3.987 Mg/m^3) and TiN (5.388 Mg/m^3: JCPDS#38-1420) without consideration for a small amount of $Al_{0.54}Ti_{2.46}N_{0.28}O_{4.58}$ phase. These data supported the ideas that during the 1st stage of HIPing the mixed powder compacts would change into pre-sintered bodies composed of Al_2O_3 matrix and TiN precipitates, and then the 2nd stage the pre-sintered bodies with only closed pores would result in dense sintered materials under high N_2 pressure at the same temperature of 1350°C (1623 K).

In the present study, two kinds of nitrogen pressure in the 2nd stage of HIPing were selected, *i.e.*, high 196 MPa and low 98 MPa as shown in Fig. 4 (a) and (b), under the expectation that SUS ball-mill-derived TiN would show poor sinter ability, on the contrary combined mill-process-derived TiN would produce dense sintered materials; the latter of which comes from common industrial viewpoints to fabricate the materials with low-cost. Therefore, the mixed powder (Al_2O_3/[Ti/$TiN_{0.3}$]) compacts from Al_2O_3 and SUS derived [Ti/$TiN_{0.3}$] were HIP sintered at 196 MPa and those contained combined-milled-process-derived [Ti/$TiN_{0.3}$] were densified at 98 MPa. Hereafter, we will call the former sintered materials as "SUS-composite materials" and the latter "WC-ZrO_2-composite materials".

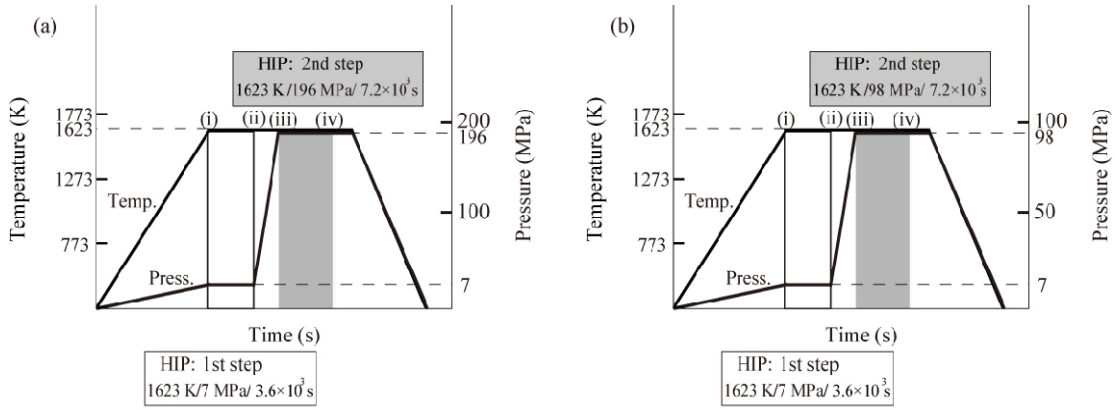

Fig. 4. Hot isostatic pressing (HIP) patterns used in the present study: the 2nd stage of HIPing was performed at (a) 196 MPa and (b) 98 MPa.

XRD pattern of the 1st HIP sintered bodies were measured; there was little difference in crystalline phase among the materials with the compositions of Al_2O_3/TiN=100/0 ~ 90/10 vol%. In addition to Al_2O_3 and TiN phases, ball-mill process-derived impurities such as, WC and ZrO_2 (Fig. 5) and $Al_{0.54}Ti_{2.46}N_{0.28}O_{4.58}$ phases were detected, the latter was explained by the solid-state reaction among Al_2O_3, $TiN_{0.3}$ and reactive Ti with absorbed oxygen on its surface during HIPing.

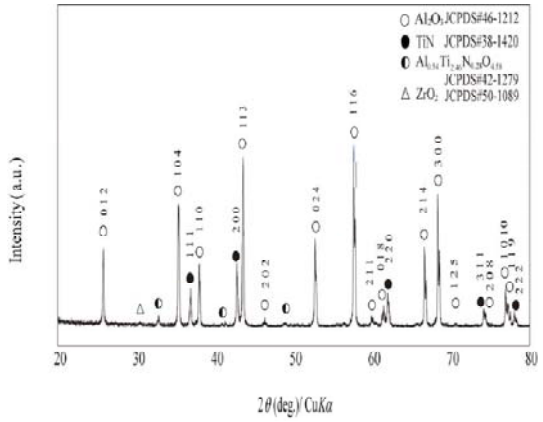

Fig. 5 X-ray diffraction (XRD) pattern of the sample after 1st stage of HIPing (1350°C [1623K]/ 7MPa/1h), in which sample has the compositions corresponding

Bulk densities of the sintered compacts ("SUS-composite materials") changed from 3.97 to 4.07 Mg/m^3 with increasing heavy TiN (5.388 Mg/m^3) content. On the contrary, their relative densities decreased from 99.6 to 98.6% as shown in Fig. 6 (a). In Fig. 6 (b) the relative densities of "WC-ZrO_2-composite materials" are also represented. The relative densities were determined based on the theoretical densities of Al_2O_3 and TiN, in calculation, the values of 15.66 Mg/m^3 (WC: JCPDS#25-1047) and 0.978 Mg/m^3 ($Al_{0.54}Ti_{2.46}N_{0.28}O_{4.58}$:JCPDS#42-1279) were ignored because of their small amounts. It should be noted that relative densities of composites ("SUS-composite materials") were higher than 98.6%, even though using a capsule-free HIPing. However, "WC-ZrO_2-composite materials" sintered at 98 MPa showed a little lower relative density as shown in Fig. 6 (b). This reduction could be explained in terms of suppression of densification for Al_2O_3 by the presence of TiN, which resulted in the reduction of grain sizes of Al_2O_3, as will be described later.

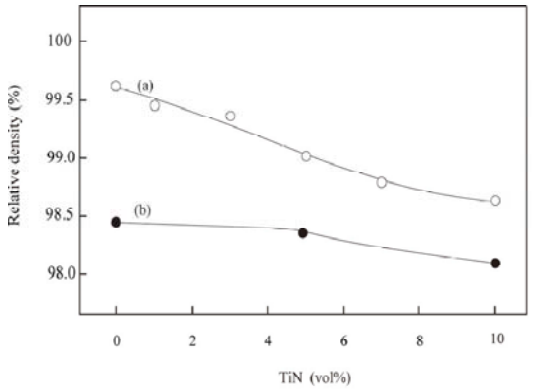

Fig. 6 Relative densities of Al_2O_3/TiN composites sintered at 1350°C (1623 K) for 2 h at N_2 pressure of (a) 196 MPa from ball-milled powders using SUS balls (10 mm^{Φ}) and (b) 98 MPa from ball-milled powders using WC ball (5 mm^{Φ}) & ZrO_2

Figure 7 presents SEM photographs for the fracture surfaces of thus prepared Al_2O_3/TiN composites containing 0, 5 and 10 vol% TiN; Fig. 7 (a) and (b) correspond to those of "SUS-composite materials" and "WC-ZrO_2-composite materials", respectively, white spots are TiN and other dark or

black grains are alumina, indicating that TiN particles are homogeneously dispersed and the grain sizes of alumina decreased as the titanium nitride content increased due to the suppression of grain growth by TiN inclusions as-mentioned before. This effect of titanium nitride is clear, when we compare the microstructures of pure alumina (100/0) and only 1 vol% TiN added (95/5) composites. Abnormal grain growth of Al_2O_3 matrix was not recognized in all the samples, revealing that homogeneously distributed TiN particles inhibited the grain growth of Al_2O_3 during HIPing. To investigate the microstructure precisely, as mentioned before, FE-TEM was utilized to observe the distribution and the cross-section of titanium nitride particles among the alumina matrix.

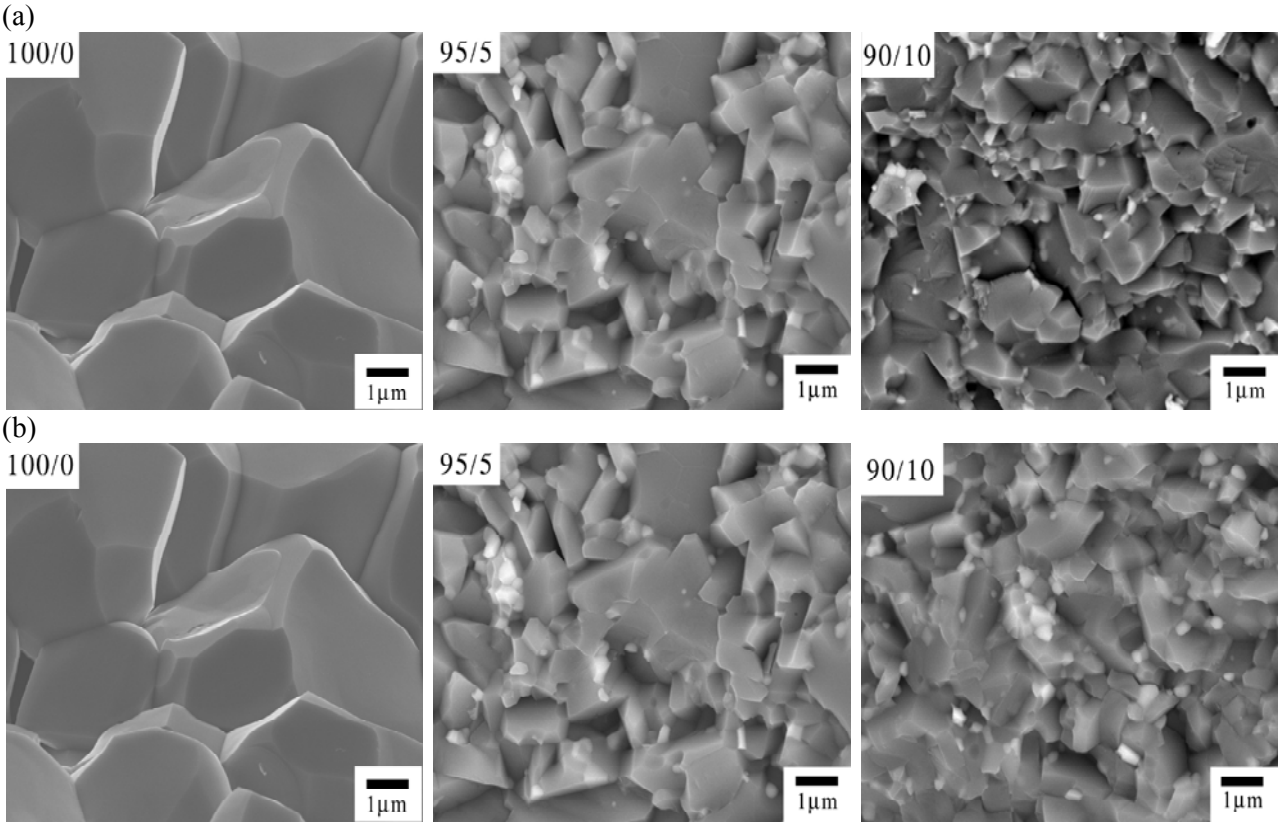

Fig. 7 FE-SEM photographs for the fracture surfaces of Al_2O_3/TiN composites containing 0,5 and 10 vol% TiN; and (b) correspond to those of "SUS-composite aterials" and "WC-ZrO_2-composite materials", respectively.

This composite (glue together) photographs (Fig. 8) are the over-view of cut and sliced specimen with the Al_2O_3/TiN=90/10 vol% composition by focused ion beam (FIB) processing; here, Fig. 8 (a) and (b) correspond to that of "SUS-composite materials" and "WC-ZrO_2-composite materials", respectively. Small black dots (inversely to the FE-SEM photograph, bright TEM image indicates light element) about 300 nm in diameter are TiN, which are distributed homogeneously at the grain boundaries, the triple-points (triple-junctions) and within the grains.

In the upper photographs in Fig 9 (a) and (b) show the black dot (particle) on the triple-points (triple-junctions) in the "SUS-composite materials" and "WC-ZrO_2-composite materials", respectively. The elemental-line analysis on the black dot is displayed under the photographs. From these, it is clear that black dots (particles) consist of only titanium and nitrogen, *i.e*., titanium nitride, from its surface to the center of dots, indicating pure monolithic TiN particle. This might be explained in terms of i) high-nitrogen pressure of 7 MPa, and ii) Al_2O_3 matrix plays a role of dilution medium, or separator for Ti particles. Therefore, even high adiabatic temperature of TiN up to 4900 K [9], strong TiN aggregates could not be formed. In Fig.10 it is observed that fine TiN particle about 100 nm exists within an Al_2O_3 grain of "WC-ZrO_2-composite materials", suggesting that combined ball-mill-derived TiN fine particles were included into Al_2O_3 matrix during their grain growth.

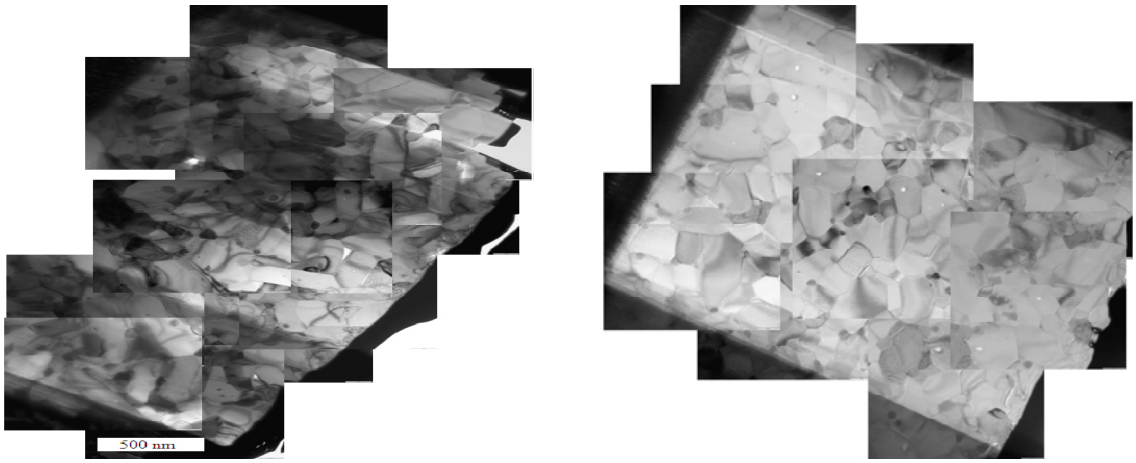

Fig. 8. FE-TEM composite (glue together) photographs of the thin-samples from Al_2O_3/TiN=90:10 vol% materials sintered at 1350°C (1623 K) for 2 h at:
(a) 196 MPaof "SUS-composite materials" and (b) 98 MPa of "WC-ZrO_2-composite materials"

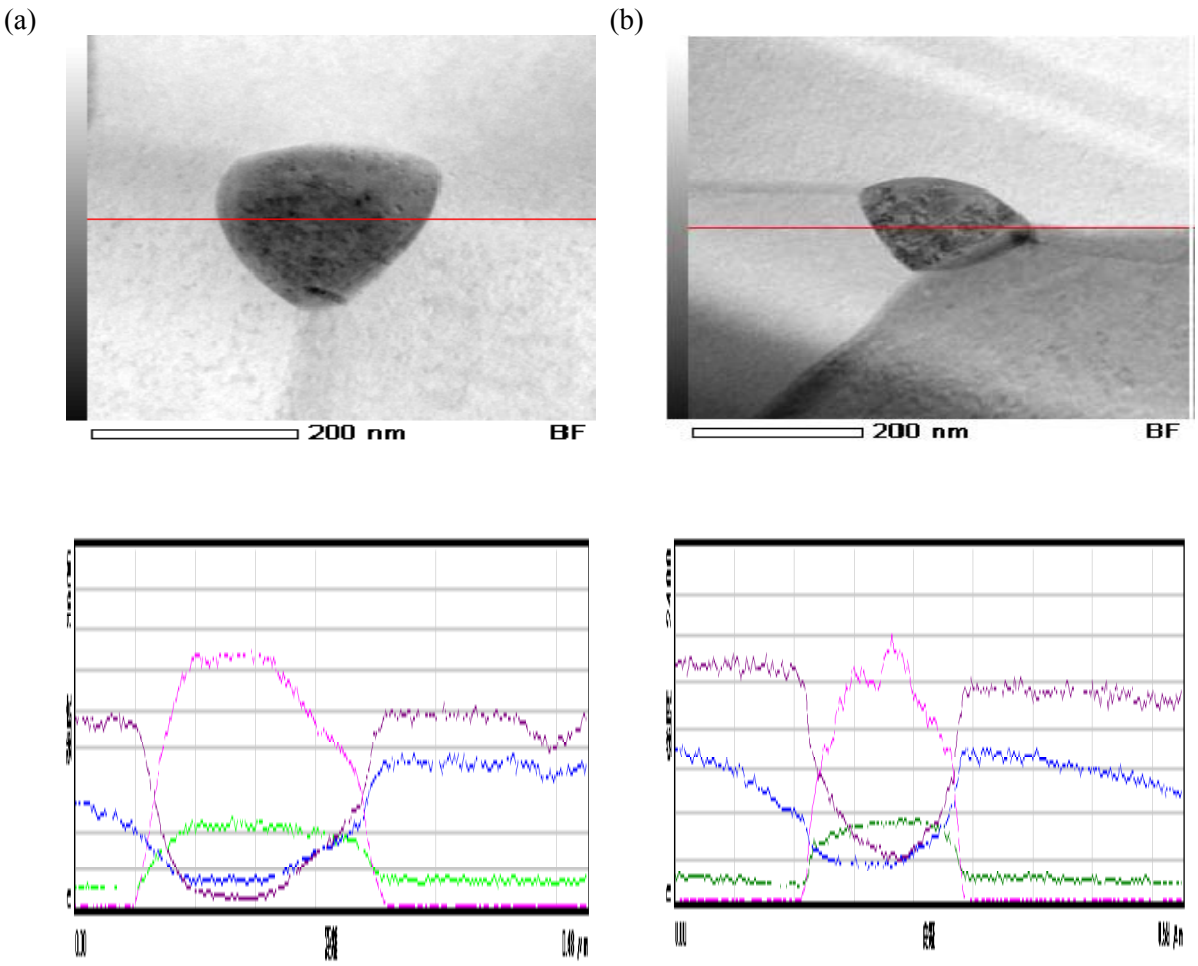

Fig. 9 Line-elemental analysis on the black particle at the triple point in Al_2O_3/TiN=90:10 vol% composite sintered at 1350°C (1623 K) for 2 h at: (a) 196 MPa of "SUS-composite materials" and (b) 98 MPa of "WC-ZrO_2-composite materials", respectively.

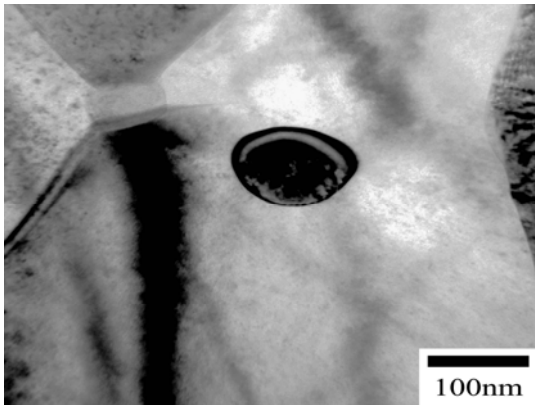

Fig.10. FE-TEM photograph showing that fine TiN particle about 100 nm exists within the Al_2O_3 grain of "WC-ZrO_2-composite materials".

From these SEM and TEM observations, grain sizes (G_s) of Al_2O_3 and TiN were estimated; in Fig. 11 (a) and (c), G^s of Al_2O_3 for both composites, respectively, decreased with increasing TiN content. Especially, between 0 and 1 vol% of TiN content, the G_s of Al_2O_3 was drastically changed from 4.0 to 1.3~1.4 μm. On the other hand, the G_s of TiN, in Fig. 11 (b) and (d) for both composites, respectively, stay almost constant valuse from 0.3 to 0.5 μm; it was clear that this size was same as $TiN_{0.3}$ and Ti as dehydrated powders, suggesting that during HIPing the grain growth of TiN was not occurred. The former might be originated from the suppression effect of small amount of TiN particles on the grain growth of Al_2O_3, even if the content of TiN was little. On the other hand, homogeneously dispersed fine metal Ti particles surrounded by vast amounts of alumina powder transformed into TiN with high enthalpy of reaction.

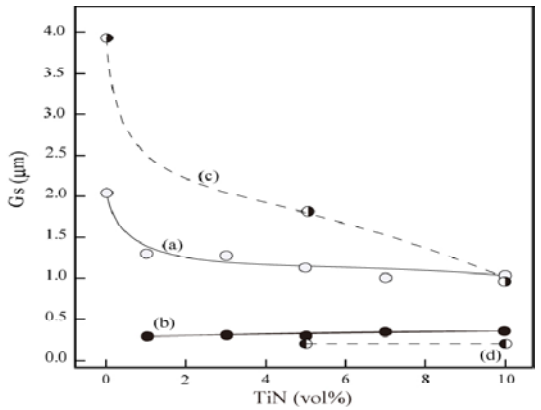

Fig. 11. Grain sizes of Al_2O_3:[(a) and (c)], and TiN:[(b) and (d)] of the sintered compacts as a function of TiN content; (a) and (b) are grain sizes of "SUS-composite materials", and (c) and (d) are grain sizes of "WC-ZrO_2-composite materials".

Mechanical and electrical properties of Al_2O_3/TiN composites

In Fig. 12 (i) and (ii), (a) three-point bending strength (σ_b), (b) Vickers hardness (H_v), and (c) fracture toughness (K_{IC}) evaluated by means of "indentation fracture (IF) method" are shown for the sintered "SUS-composite materials" and "WC-ZrO_2-composite materials", respectively. From these figures, the optimum contents of TiN to improve their mechanical properties were thought to be around 3 to 5 vol%. Especially bending strength (σ_b) had much correlation with the TiN content; for example, in the "SUS-composite materials" (Fig. 12 (i)), without TiN addition (100/0) bending strength was 525 MPa, however, a 3 vol% addition resulted in 640 MPa with a 22% increase, and then the σb value decreased to ~510 MPa.

(i)

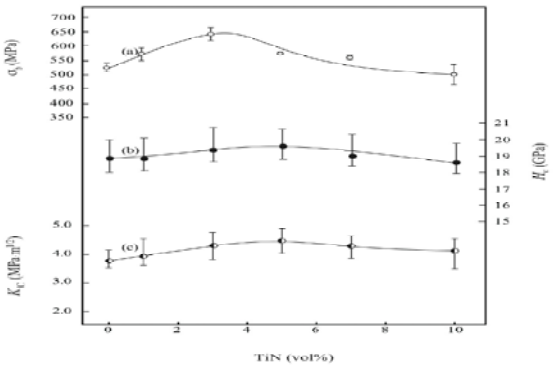

(ii)

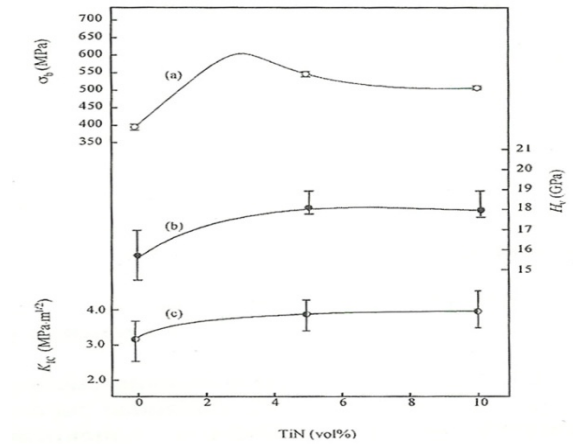

Fig. 12. Mechanical properties of Al_2O_3/TiN composites: (i) "SUS-composite materials" sintered at 196 MPa and (ii) "WC-ZrO_2-composite materials" sintered at 98 MPa. (a) Three-point bending strength (σ_b), (b) Vickers hardness H_v, and (c)

Fracture toughness (K_{IC}) was also improved from 3.8 to 4.5 MPa・$m^{1/2}$ with a 18% increase. On the other hand, hardness H_v was not changed due to the nearly same values (19 ~ 20 GPa) between alumina and titanium nitride [10]. Of course, we should take into account of reduction effect of alumina grains when we mention the H_v values of composites. In the "WC-ZrO_2-composite materials" as shown in Fig.12 (ii), in consideration with their low relative densities and a few data, there are little difference between "SUS-composite materials" and "WC-ZrO_2-composite materials".

Electrical resistivity ρ of 100/0 and 95/5 vol%Al_2O_3/TiN "SUS-composite materials" were so high that the present measuring system could not evaluate it, however, Al_2O_3/TiN = 90/10 vol% "SUS-composite materials" gave the ρ value of 2.6×103 Ω・m; this value is much lower than that (>1012 Ω・m) reported for Al_2O_3/TiN = 90/10 vol% composite fabricated by hot pressing a mixed powder compact containing ~ 1.0 μm TiN [11]. This might be explained in terms of fine 0.3 μm TiN powders used in the present study, even though the same volume fraction of TiN.

Conclusions

Highly dense sintered Al_2O_3/TiN composites with the relative density of 98.5% or more have been fabricated from the mixed powder [Al_2O_3/(Ti,$TiN_{0.30}$)] compacts directly by simultaneous synthesis and sintering using capsule-free high pressure N_2-HIPing utilizing SHS of TiN. Materials with the compositions of Al_2O_3/TiN=97/3 and 95/5vol% consisting of homogeneous Al_2O_3 (2.0-1.3 μm) matrix and fine TiN particles (~0.3 μm) distributed uniformly among the Al_2O_3 matrix gave higher mechanical properties than those of monolithic alumina. From the results of the present study, it has been cleared that by applying capsule-free N_2-HIPing to the preparation of engineering ceramics containing metal-nitride, which nitride is even difficult to be synthesized under the conventional conditions, this process provides the low-cost fabrication method with easy handling in a short operation time.

And thus prepared metal nitrides will provide a new wide application field in future.

Acknowledgement

The authors wish to thank Dr. T. Fujii, Industrial Research Center of Shiga Prefecture in Japan for his offer of ball-milled fine TiH_2 powders. The authors thank Ms. M. Toda and Ms. J. Morita of the Doshisha University Research Center for Interfacial Phenomena, for FE-SEM and Fe-TEM observations of the samples.

References

1. Sheriff M., Eskandarany El., Omori M., Sumiyama K., Hirai T., Suziki K. Plasma Activated Sintering for Consolidation of Mechanically Reacted TiN powder. *J. Jpn. Soc. Powder Powder Metal*., 44, 547-553 (1997).
2. Gogotsi Y.G., Porz F., "Mechanical properties and oxidation behavior of Al_2O_3-AlN-TiN composites" *J. Am. Ceram. Soc*., 75, 2251-2259 (1992).
3. Mocellin A., Bayer G., "Chemical and microstructural investigation of high-tenperature interaction AlN and TiO_2" *J. Mater. Sci*., 20, 3697-3704 (1985).
4. Rak Z.S., Czechowski J. "Manufacture and Properties of Al_2O_3-TiN Particulate Composites," *J. Eur. Ceram. Soc*., 18, 373-380 (1998).
5. Yamada O., Hachiya M., Nakane S., Yoshinaka M., Hirota K., Yamaguchi O., "Simultaneous Synthesis and Sintering of α-Ti(N) by Self-propagating High-temperature Combustion under Nitrogen Pressue", *J. Mater. Sci. Lett*., 18[5]363-365 (1999).
6. Kubo K., Hitomi A., "Fabrication of Al_2O_3-TiN Micro-composite Derived from TiO_2 Precursor", *J. Jpn. Soc. Powder Powder Metal*., 53, 323-328 (2006).
7. Mendelson M.I., "Average Grain Size in Polycrystalline Ceramics", *J. Am. Ceram. Soc*., 52, 443-446 (1969).
8. Niihara K., Morena R., Hasselman D.P.H., "Evaluation of *K*IC of Brittle Solids by the Indentation Method with Low Crack-to-Indent Ratios", *J. Mater. Sci. Lett*., 1, 13-16 (1982).
9. Subrahmanyam J., Vijayakumar M., "Review Self-propagating high-temperature synthesis", *J. Mater. Sci*., 27, 6249-6273 (1992).
10. Lackey W.J., Stinton D.P., Cerny G.A., Schaffhauser A.C., Fehrenbacher L.L., "Ceramic Coatings for Advanced Heat Engines – A Review and Projection", *Adv. Ceram. Mat*., 2[1]24-30(1987).
11. Rak Z.S., Czechowski J., "Manufacture and Properties of Al_2O_3-TiN Particulate Composites", *J. Eur. Ceram. Soc*., 18, 373-380 (1998).

Received 9 August 2010